JOURNAL OF SOLID STATE CHEMISTRY 45, 1–13 (1982)

Electrical Transitions in Metal Oxides*

J. M. HONIG

Department of Chemistry, Purdue University, West Lafayette, Indiana 47907

Received April 23, 1982

A discussion of various electrical and magnetic transitions is provided for the cases of Fe_3O_4, V_3O_5, and V_2O_3. The different mechanisms responsible for these transitions are briefly outlined.

Introductory Comments

Electrical transitions in metal oxides have been extensively studied for over three decades and reviewed several times (*1, 2*); however, there still is no agreement on the basic mechanisms that induce such transformations in specific cases. We examine here recent findings for three systems, Fe_3O_4, V_3O_5, and V_2O_3, as being representative of current studies.

The Verwey Transition in Magnetite, Fe_3O_4

Recent work in this area has been summarized in a topical conference (*3*). Magnetite undergoes several transitions: it has a Néel point near 850K, below which it exhibits ferrimagnetic ordering. A second transformation near T_V = 123K is the so-called Verwey transition: This is not a metal–insulator transformation; rather, the material is a semiconductor both above and below T_V. Additional, less dramatic, changes in properties have also been occasionally observed at 200 and at 12K.

Here we consider only the Verwey transition. The material crystallizes in the inverse spinel structure: Fe^{2+} and half of the Fe^{3+} ions are located on octahedral interstices (B-type sites) in the oxygen network; the remaining Fe^{3+} are located on tetrahedral (A-type) sites.

Detailed structural studies, via neutron diffraction (*4–7*) and nuclear magnetic resonance (*8, 9*), show that charge ordering of Fe^{2+} and Fe^{3+} and thereby, long-range order (l.r.o.) is established below T_V. As is lucidly explained by Cullen (*10*), on alternate $(00\bar{1})$ planes cation strings run along the $[\bar{1}10]$ or [110] directions, labeled as *a* or *b* chains (or strings), respectively. Along one *a* chain three Fe^{2+} ions in succession are followed by one Fe^{3+} unit; at corresponding locations on an adjacent *a* chain three Fe^{3+} ions are succeeded by one Fe^{2+} unit. In principle, cationic ordering also occurs on each *b* chain, involving a pair of Fe^{3+} ions, followed by a pair of Fe^{2+} ions in alternation. However, as stressed by Cullen (*10*) and by Iida (*11*), successive *–b–a–b–* planes perpendicular to the *c* axis are stacked such that proximate cations in three successive planes can be grouped into

* Presented at the Symposium on the Electronic Structure and Bonding in Solids, 183rd National Meeting, American Chemical Society, held in Las Vegas, Nevada, March 29–30, 1982.

0022-4596/82/130001-13$02.00/0

hexagonal ring patterns involving Fe^{2+} and Fe^{3+} in alternation. In this type of charge ordering all cations along b strings are members of rings, whereas only a quarter of the a-string cations are involved in ring formation. The synchronous displacement of three electrons to their nearest-neighbor position inside any ring produces an interchange of Fe^{2+} with Fe^{3+}, i.e., in a reversal of charge configuration, at very small net cost in energy. At any time, a significant fraction of hexagonal rings exists in the "inverted" charge configuration, thus randomizing charge along the b strings, but leaving three quarters of the a-chain constituents in an ordered arrangement below the Verwey transition. This rationalizes earlier experimental findings that it is the a-plane cations which order and which propagate l.r.o. at low temperatures.

Coulomb interactions are not the only forces involved in the ordering for $T < T_V$. The existence of superstructure lines just above T_V in critical neutron scattering (*5*) and the detailed investigation of elastic and inelastic neutron scattering (*7*) reveal the existence of a soft mode with wave vector $\mathbf{k} = (00\xi)$ that "condenses" at $\mathbf{k} = (00\frac{1}{2})$. This must be understood in terms of the ordering along the z axis. As one proceeds from one Fe^{2+} or from one Fe^{3+} ion in the a plane at $z = \frac{1}{8}$ to the corresponding position in the a plane at $z = \frac{9}{8}$ one arrives at the complementary charge, namely, Fe^{3+} or Fe^{2+}, respectively. One must advance by twice the unit lattice distance along c to duplicate the same ionic configuration at $z = \frac{17}{8}$ that prevails at $z = \frac{1}{8}$. Formally, this corresponds to the existence of a charge density wave (CDW) with wavelength $\lambda = 2c$. This CDW couples strongly to the corresponding phonon mode with the same wave vector. At the transition the ordering of the charges leading to the establishment of the CDW occurs simultaneously with phonon condensation, producing a net atomic displacement that lowers the symmetry.

The general features of such a phase transformation may be simulated by the pseudospin formalism sketched out below, following the lucid discussion of Yamada (*12*). Any two-state system may be described by wave functions of the form $\phi_0 = \begin{pmatrix}0\\1\end{pmatrix}$ and $\phi_1 = \begin{pmatrix}1\\0\end{pmatrix}$; the energy difference associated with these states is labeled $\Delta\epsilon \equiv \epsilon_g$. For such a case the Hamiltonian of the unperturbed system may be written as

$$\mathcal{H}_g = \frac{\epsilon_g}{2}\begin{pmatrix}1 & 0\\0 & -1\end{pmatrix} \equiv \frac{\epsilon_g}{2}\hat{\sigma}_z. \tag{1}$$

For using straightforward matrix multiplication one obtains the ground-state energy as

$$\mathcal{H}_g\phi_0 = \frac{\epsilon_g}{2}\begin{pmatrix}1 & 0\\0 & -1\end{pmatrix}\begin{pmatrix}0\\1\end{pmatrix} = -\frac{\epsilon_g}{2}\begin{pmatrix}0\\1\end{pmatrix}, \tag{2a}$$

and the excited state energy as

$$\mathcal{H}_g\phi_1 = \frac{\epsilon_g}{2}\begin{pmatrix}1 & 0\\0 & -1\end{pmatrix}\begin{pmatrix}1\\0\end{pmatrix} = +\frac{\epsilon_g}{2}\begin{pmatrix}1\\0\end{pmatrix}, \tag{2b}$$

which shows that the energy difference is indeed $\Delta\epsilon = \epsilon_g$, as claimed.

One can next introduce a perturbation operator via

$$\mathcal{H}_t \equiv Fe^{i\omega t}\begin{pmatrix}0 & 1\\1 & 0\end{pmatrix} \equiv Fe^{i\omega t}\,\hat{\sigma}_x, \tag{3}$$

where $Fe^{i\omega t}$ is a sinusoidally varying "field" of amplitude F and angular frequency ω. It may readily be checked by the same matrix algebra that

$$\mathcal{H}_t\phi_0 = Fe^{i\omega t}\,\phi_1, \tag{4}$$

$$\mathcal{H}_t\phi_1 = Fe^{i\omega t}\,\phi_0, \tag{5}$$

which shows that the operator $\mathcal{H}_t$ in (3) describes the changeover from (i.e., induces a transition from) state ϕ_0 into state ϕ_1, and vice versa.

As indicated in (1) and (3), $\mathcal{H}_g$ and $\mathcal{H}_t$ are proportional to the conventional Pauli spin matrix representations (or spin operators) $\hat{\sigma}_z$

and $\hat{\sigma}_x$. Hence one may formally represent any two-state system as a collection of pseudospins and apply to these the full panoply of theoretical knowledge concerning magnetic ordering. At the simplest level one introduces the well-known Heisenberg Hamiltonian (see, for example, Ref. (*13*)) in the presence of an externally applied magnetic field,

$$\mathcal{H}_H = -\sum_{i\neq j}\sum J_{ij}\hat{\mathbf{S}}_i \cdot \hat{\mathbf{S}}_j - g\mu_B H \sum_i S_i^z, \quad (6)$$

where J_{ij} is the exchange integral, $\hat{\mathbf{S}}_i$, $\hat{\mathbf{S}}_j$, and S_i^z are the total spin operators for sites i and j and the z component of said operator on site i, $g(\sim 2)$ is the electronic g factor, μ_B is the Bohr magneton, and H is the applied magnetic field. If one focuses on a specific site i, then $\mathcal{H}_i = -\hat{\mathbf{S}}_i \cdot \left(\sum_i J_{ij}\hat{\mathbf{S}}_j + g\mu_B H\hat{\mathbf{z}}\right)$ has the *form* of a spin operator $\hat{\mathbf{S}}_i$ in an effective magnetic field of magnitude

$$H_e \equiv H + (g\mu_B)^{-1}\sum_{j(\neq i)} J_{ij}|\hat{\mathbf{S}}_j|. \quad (7)$$

One now simplifies the derivation by replacing the operator $\hat{\mathbf{S}}_j$ with its expectation value $\langle\hat{\mathbf{S}}_j\rangle$, which is related to the magnetization $\mathcal{M} = g\mu_B\langle\hat{\mathbf{S}}_j\rangle$. Equation (7) may now be recast in the form

$$H_e = H + (g\mu_B)^{-2}\sum_{j(\neq i)} J_{ij}\mathcal{M} \equiv H + \lambda\mathcal{M}, \quad (8)$$

wherein $\lambda \equiv (g\mu_B)^2 J_0$ and $J_0 \equiv \sum_{j(\neq i)} J_{ij}$.

In the present approximation we may then express the magnetization via

$$\mathcal{M} = \mathcal{M}_0(H_e), \quad (9)$$

where $\mathcal{M}_0$ is the magnetization calculated in the absence of any interactions among magnetic moments, but with H replaced by H_e. One can thus determine the susceptibility χ according to

$$\chi \equiv \partial\mathcal{M}/\partial H = (\partial\mathcal{M}_0/\partial H_e)(\partial H_e/\partial H) = \chi_0(1 + \lambda\chi), \quad (10)$$

wherein $\chi_0 \equiv \partial M_0/\partial H_e$; the second factor on the right follows from use of Eq. (8). Equation (10) may be solved for

$$\chi = \chi_0/(1 - \lambda\chi_0), \quad (11)$$

showing that the susceptibility becomes unbounded when $\lambda\chi_0 \to 1$. As is well known this corresponds to the onset of magnetic ordering and involves a phase transition. The above scheme is very primitive but it conveys the essence of the general approach; much more sophisticated formulations of cooperative phase transitions have been developed.

While a reasonably satisfactory structural characterization of the Verwey transition has been achieved, many details remain to be settled: for example, the structure of the low-temperature phase which has been variously labeled as rhombohedral, orthorhombic, monoclinic, or triclinic; the actual deviations from the strictly cubic spinel configurations are slight, making it difficult to characterize the structure correctly. Iida (*1*) has summarized at length the current understanding of atomic configurations at the Verwey transformation.

The electrical characteristics of Fe_3O_4 both above and below T_V are less well understood. First, there is no unanimity concerning the conduction mechanism. Cullen and Callen (*16*) assumed charge carrier itineracy, though the data cited in support of their model (*17–19*) do not unambiguously support such a view. Most workers invoke the small polaron model in their analysis. The resistivity and thermoelectric studies by Kuipers and Brabers (*20*) on carefully annealed single crystals are consistent only with a small polaron model. Their data are in reasonable agreement with

those of Graener *et al.* (*21*) on untreated crystals.

Second, there is confusion about the variation of the conductivity σ of Fe_3O_4 with temperature. Thus McKinnon *et al.* (*22*) and Shiozaki *et al.* (*23*) cite earlier publications and their own work to assert that, at least for $T_V/2 \lesssim T < T_V$, the conductivity does not follow an Arrhenius law, but conforms better to the relation $\sigma \sim \exp(T/T_0)$. These findings are interpreted as indicating incoherent tunneling of electrons between adjacent atomic sites. Graener *et al.* (*21*), on the other hand, claim that for $40 < T < 123$K their data best fit the relation $\log \sigma \sim T^{-1/4}$, appropriate to the variable range hopping mechanism of Mott. Data recently taken in the range 77–520K at the author's laboratory on thoroughly annealed single crystals conform strictly to the Arrhenius equation or to a relation of the form $\log(\sigma T^{1/2}) \sim 1/T$. Three absolutely straight line regions were encountered as indicated in Table I, which lists the conductivity activation energies. At 123K there occurs a discontinuity in resistivity of nearly 2 orders of magnitude, along with a sudden change in conductivity activation energy. At 200K there is found an extremely sharp change in slope of the Arrhenius plot without a discontinuity in σ.

One must now ask with Mott (*14, 15*) why, if long-range order is lost on heating Fe_3O_4 through the Verwey transition, the resistivity *decreases* by 2 orders of magnitude. Ihle and Lorenz (*24*) have suggested

TABLE I

LISTING OF CONDUCTIVITY ACTIVATION ENERGIES ϵ_σ FOR Fe_3O_4 SINGLE CRYSTALS

Temperature range	ϵ_σ (eV)
Below T_V = 123K	0.110
123–200K	0.0438
Above 200K	0.0074

that for $T < T_V$ the allowed states for B-type electrons fall into two very narrow energy ranges separated by a gap that is generated by Hubbard-type correlation effects. At the Verwey temperature the suppression of l.r.o. also induces a change in short-range order. This introduces energy states in the midgap range, close to the position of the Fermi level. The activation energy for generation of charge carriers now vanishes and the charge carrier density is drastically altered. In this model the conductivity activation energy for $T > T_V/2$ also represents the mobility activation energy.

This scheme derives considerable support from thermoelectric measurements (*19–21*). The recent work of Kuipers and Brabers (*20*) is reproduced in Fig. 1; these authors interpret their data below the Verwey transition in terms of two types of polarons, electron- and hole-like, which populate the two sets of energy levels. The need for a two-level scheme is evident even on a qualitative basis, in view of the change in sign of α at low temperatures. Standard theory (see also Ref. (*26*)) leads to the following relation for the total Seebeck coefficient of a two-level small polaron conductor:

$$\alpha = \frac{1}{eT}\left[\frac{-n_n(\Delta - \epsilon_F) + n_p(\Delta + \epsilon_F)(u_n/u_p)}{n_n + n_p(u_n/u_p)}\right], \quad (12)$$

in which e is the electronic charge, n_n and n_p are the charge carrier densities in the upper and lower set of levels, respectively, 2Δ is their separation on the energy scale, and u_n and u_p are the polaron mobilities given by

$$u_n = u_n^0 e^{-\epsilon_n/kT}, \qquad u_p = u_p^0 e^{-\epsilon_p/kT}, \quad (13)$$

in which u_n^0 and u_p^0 are very weak functions of temperature and ϵ_n, ϵ_p are mobility activation energies. As shown in Fig. 1, the α values for $T < T_V$ can be reproduced very well by selecting an energy gap $2\Delta = 0.12$ eV, $u_n^0 \approx u_p^0$ and $\Delta\epsilon \equiv \epsilon_p - \epsilon_n = 0.007$ to

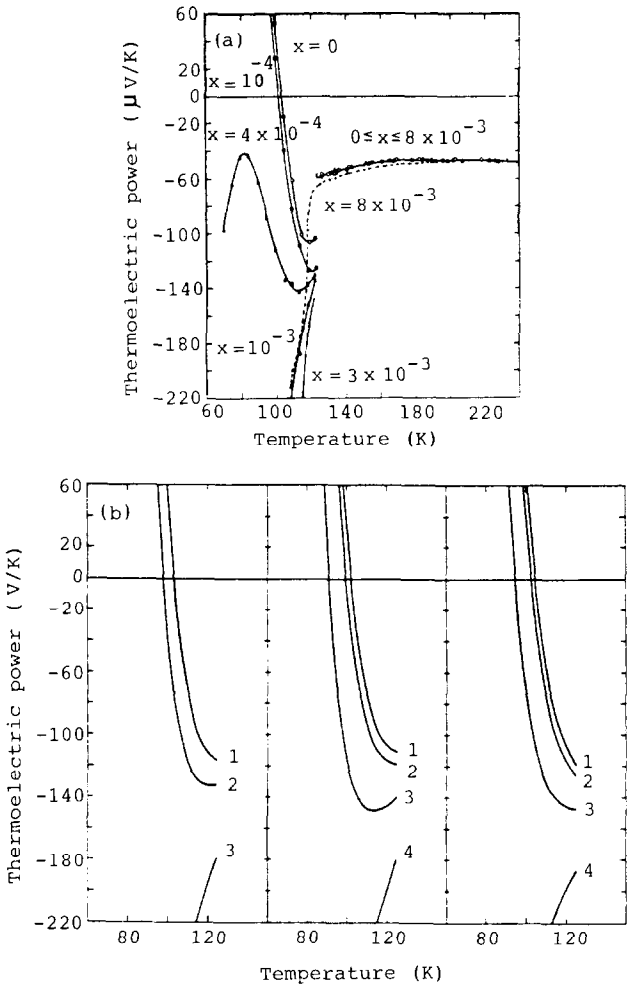

FIG. 1. Seebeck coefficients for annealed single crystals of $Fe_{3-x}Ti_xO_4$, $0 \leq x \leq 8 \times 10^{-3}$. (a) Experimental results. (b) Theoretical calculations based on Eq. (12) for various values of the parameters Δ, u_n/u_p, and stoichiometry. After Ref. (*20*). (1) $x = 0$, (2) $x = 10^{-4}$, (3) $x = 4 \times 10^{-4}$, (4) $x = 10^{-3}$.

0.008; n_n and n_p as well as ϵ_F are related to the deviations from strict stoichiometry by an octahedral vacancy concentration of roughly 5×10^{-4}.

Above the Verwey transition the near-constancy of the Seebeck coefficient noted by all investigators is readily explained in terms of a constant density of charge carriers; a modified version of the Heikes formula is then applicable in the expression for α. Such a situation could arise either if the 2Δ gap collapsed completely above T_V, as suggested by Kuipers and Brabers, or if additional levels were generated at $\epsilon = \epsilon_F$, as in the model of Ihle and Lorenz. A more complex interpretation of the $\alpha(T)$ variation over the entire range of measurements has been advanced by Mott (*14, 15*).

The nature of the σ anomaly at 200K is unclear. In all prior conductivity measurements this very sharp change in $d \log \sigma/dT$ is replaced by a gradual change in this slope or, in some of the early measurements, by a maximum of σ in the vicinity of that temperature. Further experimental work is re-

quired for an understanding of the high-temperature properties of Fe_3O_4.

The Electrical Transitions in V_3O_5

V_3O_5 is a member of the Magnéli series V_nO_{2n-1} ($3 \leq n \leq 10$) which is obtained from the rutile VO_2 structure by ordered omission of chains of oxygen atoms, and by crystal shear along $(1\bar{2}1)$, as illustrated in Ref. (*27*). Formally, the new arrangement may be viewed as a string of n rutile blocks, separated by a distorted V_2O_3 unit. In V_3O_5 nuclear magnetic resonance studies (*28*) provide no evidence of the spin-pairing of cations in the three-unit chain that is prevalent among the longer chains of the higher homologs.

V_3O_5 undergoes two transformations near T_t = 425K and T_N = 76K, respectively; earlier reports of additional transitions at 130, 175, or 235K may be linked (*29*) to the presence of other Magnéli phases as contaminants in the specimens under study. The low-temperature transformation at T_N = 76K is accompanied by antiferromagnetic ordering, as detected by ^{51}V nmr (*28*), by Mössbauer measurements on ^{57}Fe-doped specimens (*30*), and by spin-flip neutron-scattering experiments (*31, 32*). There is divergence of opinion on the nature of the high-temperature transition: the electrical measurements, reviewed in Ref. (*33*), appear to be consistent with semiconducting behavior both above and below T_t. However, the optical measurements of Terukov *et al.* (*34, 35*) indicate clearly that for $T > T_t$, V_3O_5 exhibits strong infrared reflectivity and a plasma edge, whereas for $T < T_t$ lattice vibrational bands are observed in the range 0.05 to 0.25 eV. These findings provide strong evidence for a metal–insulator transition at $T = T_t$. The small, negative slope of $d\rho/dT$ for $T > T_t$ may be rationalized by postulating the type of band overlap observed in the related cases of V_2O_3 (*36, 37*) and VO_2 (*38*). If band overlap decreases with diminishing temperature, the charge carrier density within the electron and hole pockets changes correspondingly, thus increasing the resistivity.

The change of magnetic susceptibility χ with temperature is shown in Fig. 2. Note that beyond the maximum χ obeys the Curie–Weiss law, as shown in the insert, and changes very little at the transition T_t. While such a T dependence is frequently taken as an indication of electron localization, the Curie–Weiss law is also consistent with itinerant electrons in narrow d-band states, such as postulated for V_3O_5.

In recent X-ray crystallographic studies (*39, 40*) below T_t many very weak reflections have been detected; these indicate slight deviations from the centered monoclinic atomic arrangement. The changes in the diffraction patterns on passing through the transition temperature T_t are very minor (*41–44*). No information seems to be available concerning structural changes at the Néel temperature, T_N.

Recent work (*45, 46*) on the heat capacity (C_N) anomaly at the Néel temperature is shown in Fig. 3. Three features are noteworthy: first, the entropy of transition, 0.29 J/K-mole V_3O_5, is only 1.3% of the value $\Delta S_N = R(2 \ln 3 + \ln 2) \simeq 24$ J/K-mole V_3O_5 calculated on the assumption of complete magnetic disordering and of total charge differentiation with respect to V^{3+} and V^{4+} ions. Second, considerable magnetic short-range order persists far above the Néel point, as judged by the nature of the heat capacity curve in the range $T_N < T < T_t$ (*29*). Third, the maximum in magnetic susceptibility occurs at a much higher temperature, $T_m \sim 125$K, than the actual transition $T_N \sim 76$K, as indicated by the maximum in C_N.

The above features are all interpretable in terms of the fundamental analysis by Fisher (*47, 48*) (see also (*49*)) if one accepts the concept that lower-dimensional magnetic ordering prevails for $T_N \leq T \leq T_t$ in V_3O_5.

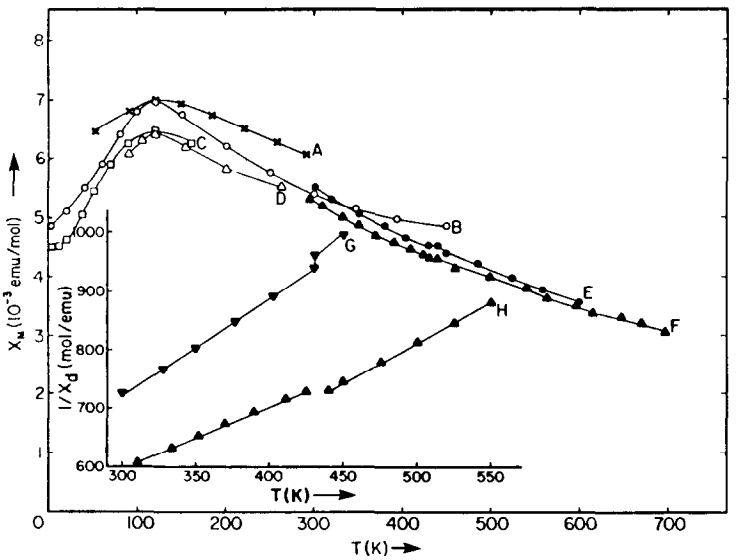

FIG. 2. Variation of magnetic susceptibility with temperature for V_3O_5, as determined by various investigators. After Ref. (*33*).

This is rendered plausible by the crystal structure in which chains of three unpaired vanadium ions separated by jogs run along the pseudorutile *b* axis.

As explained by de Jongh and Miedema (*49*), in a truly one-dimensional material no long-range order prevails above $T = 0$. The magnetic entropy is thus tied exclusively to existing short-range order. This is manifested in the variations of the excess magnetic specific heat C_N and of the magnetic susceptibility χ with temperature. Theoretical analysis (*48*) indicates for the Heisenberg chain that C_N starts from zero at $T = 0$ and builds up to a broad maximum in the range $0.5 < kT/|J|S(S + 1) < 1.3$; here J is the intrachain magnetic exchange energy for adjacent centers. C_N thereafter drops only very gradually with rising temperature. The magnetic susceptibility, on the other hand, has a finite intercept at $T = 0$ whose value lies in the range $0.6 < 2|J|\chi/N_0g^2\mu_B^2 < 1.5$; here N_0, g, and μ_B are Avogadro's number, the electronic g factor, and the Bohr magneton, respectively. χ peaks in the range $1 < kT/|J|S(S + 1) < 1.7$ and drops off only very slowly with rising temperature.

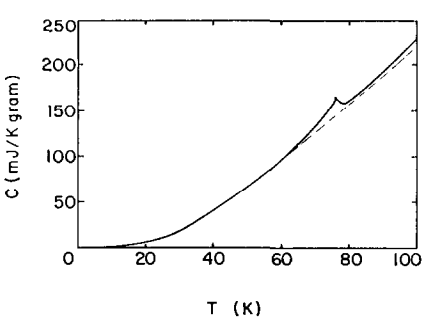

FIG. 3. Variation of heat capacity with temperature for single crystals of V_3O_5, showing the anomaly at T_N = 76K. Dotted curve represents estimated baseline. After Ref. (*46*).

Since no real material is truly one-dimensional, the properties of a linear chain may be approximated in materials where the ratio J'/J is very small, J' being the interchain magnetic exchange energy for adjacent chains. Even for ratios J'/J as small as 0.01, the heat capacity anomaly C_N consists of a superposition of the broad maximum at $T = T_0$ for a truly one-dimensional material, and

of a sharp spike at temperature $T_N < T_0$; the smaller the ratio J'/J the lower is T_N. For $T > T_N$ the heat capacities corresponding to $J' = 0$ and $J' \neq 0$ merge indistinguishably, whereas for $T < T_N$, C_N for $J' \neq 0$ drops off to zero much more sharply than does C_N for a strictly one-dimensional chain. These facts reflect the existence of long-range order for $T < T_N$ and $J'/J > 0$, no matter how weak the interchain exchange coupling, and the occurrence of short-range order to temperatures well above T_0. This explains the anomalously low entropy change encountered at the $T_N = 76$K transition.

The magnetic susceptibility variation is much less drastically affected by turning on magnetic interchain coupling. The smooth variation of χ with T for truly one-dimensional materials should give way to a mild cusp-like anomaly near $T = T_N$ when $J' > 0$. However, this feature may remain undetected unless a specific search for the anomaly is carried out. The relationship between C_N and χ will be further commented upon below.

On the basis of structural arguments and through the Oguchi relation for the related rutile-type structure, the ratio J'/J for V_3O_5 has been estimated (*46*) to lie in the range 0.06 to 0.1 for $S = \frac{1}{2}$ and $S = 1$, respectively. Thus V_3O_5 would appear to qualify as a pseudo one-dimensional material. In fact, Figs. 2 and 3 show a close resemblance to the theoretical curves for C_N and for χ of one-dimensional materials. Here, it must be borne in mind that C_N is an excess heat capacity, obtained by subtraction of the background. As specifically emphasized in Ref. (*29*), the high-temperature heat capacity measurements show up the persistence of short-range order well beyond 300K; this feature is not readily detectable in the limited data set of Fig. 3. The excess heat capacity quickly drops toward zero as the temperature is lowered away from T_N. Also, the magnetic susceptibility exhibits the anticipated variation with temperature for pseudo one-dimensional materials.

There is a second criterion that must be met by materials of low dimensionality, namely, that the temperature at which C_N exhibits a spike (at T_N) and χ passes through a maximum (at T_m) should differ considerably. This fact may be understood on the basis of very general arguments presented by Fisher (*47, 48*) which lead to the following interrelation

$$C_N = A\, \partial(\chi_\parallel T)/\partial T, \tag{14}$$

in which A is a slowly varying function of temperature.

A simplified derivation proceeds as follows: In the absence of an externally applied magnetic field ($H = 0$) the Heisenberg Hamiltonian (6) may be written as

$$\mathcal{H} = \sum_{i=1}^{N} \sum_{j=1}^{qj} J_{ij}(S_i^z S_j^z + S_i^x S_j^x + S_i^y S_j^y), \tag{15}$$

where the minus sign has been absorbed in J_{ij}. We now restrict the j summation to the q nearest neighbors of site i, by setting $j = 1$; we then sum over all N lattice sites and replace J_{i1} by $|J|$. We next take the expectation value of the resulting expression; this represents the magnetic energy U_M of the assembly in the above approximation:

$$\begin{aligned} U_M &= N|J|q\,[\langle S_0^z S_1^z\rangle + \langle S_0^x S_1^x\rangle + \langle S_0^y S_1^y\rangle] \\ &= 3\,Nq|J|\,\langle S_0^z S_1^z\rangle. \end{aligned} \tag{16}$$

As is well established, the magnetic susceptibility is given by

$$\begin{aligned} \chi &= (Ng^2\mu_B^2/kT) \sum_j \langle S_0^z S_j^z\rangle \\ &\simeq (Ng^2\mu_B^2 q/kT)\,\langle S_0^z S_1^z\rangle. \end{aligned} \tag{17}$$

On the right we have also restricted the summation in (17) to the q nearest neighbors. Elimination of $\langle S_0^z S_1^z\rangle$ between (17) and (16) and differentiation of U_M with re-

spect to T now yields

$$C_N = \frac{3|J|k}{g^2\mu_B^2}\frac{\partial}{\partial T}(\chi T) \equiv A\frac{\partial}{\partial T}(\chi T) \quad (18)$$

as claimed earlier. This very simple derivation agrees within several factors of unity with the results derived by more elaborate techniques (*47, 48*). The primary objective is to rationalize the proportionality between C_N and $\partial(\chi T)/\partial T$.

One can now appreciate that in two- or three-dimensional materials for which C_N is sharply spiked at $T = T_N$, $\partial(\chi T)/\partial T$ as well as $\partial\chi/\partial T$ become essentially infinite. This means that the maximum in χ vs T, $\chi(T_m)$, must be at some temperature T_m slightly in excess of T_N. However, for a one-dimensional chain C_N passes through a very broad maximum; the slope of $\chi(T)$ is now much smaller than before; correspondingly, the maximum in χ now occurs at a temperature T_m considerably higher than T_N. The predicted ratio of T_m/T_N lies in the range 1.33 to 1.5 for Heisenberg chains with $S = \frac{1}{2}$ and 1, respectively. This quantity varies with the detailed magnetic interactions that are adopted. The experimental value for V_3O_5 is approximately 1.6, which is somewhat too large to fit comfortably, but there are several mitigating factors. First, it is difficult to locate the quantity T_m exactly from the very broad maximum in the experimental data; a reduction of T_m from 125 to 115K would bring the temperature ratio toward the theoretical upper limit. Second, the spike in C_N is always at a lower temperature than the broad maximum encountered at T_0 in a truly one-dimensional material. Hence, T_N as read off from the spike lies below the value T_0 where the broad maximum in C_M is found. Lastly, T_m/T_N is sensitive to the type of magnetic interaction that is assumed. For an Ising chain the theoretical limits T_m/T_N range between unity and 2.4, depending on spin and on whether one deals with the quantity $\chi_\parallel$ or $\chi_\perp$. In any event, it is clear that the observed T_m/T_N for V_3O_5 is far below the value anticipated for ordinary three-dimensional compounds.

In summary, the very broad maximum in χ vs T, the shallow heat capacity spike superposed on a much broader background anomaly, the large ratio of T_m/T_N and of J/J', and the very small value of ΔS_N at T_N are all consistent with the hypothesis that the transition at $T = T_K \approx 76$K reflects a changeover from three- to pseudo one-dimensional chain ordering in V_3O_5. The transition at $T = 430$K then represents a metal–insulator transformation; the mechanism responsible for this latter change is still not clear.

Electrical Transitions in the V_2O_3 Alloy System

The electrical characteristics of the alloy system $(V_{2-x}M_x)_2O_3$, M = Cr, Al, Ti, have been repeatedly investigated. Work in this area before 1975 is reviewed in Ref. (*1*); research since then is found in Refs. (*50–56*). The system is of considerable interest because it exhibits a set of spectacular metal–insulator transitions sketched schematically in Fig. 4 as plots of log ρ vs $1/T$. The following regimes may be distinguished:

I. Pure V_2O_3 at lowest temperatures is an antiferromagnetic insulator (AFI) which, in the temperature range $T = 160$–170K, exhibits a transition to a very high resistivity metal; beyond approximately 350K the resistivity rises anomalously by a factor of 3 and then becomes constant above 800K. $(V_{2-x}M_x)_2O_3$ alloys, with M = Cr, Al and $0 < x < 0.005$, follow the same general pattern.

II. $(V_{2-x}M_x)_2O_3$ alloys, with M = Cr, Al and $0.005 < x < 0.018$, are subject to three transitions on heating: the first is a transformation from an antiferromagnetic insulator (AFI) to a metallic (M) phase in the range 160–180K; the transition temperature rises with increasing x. The second is a sudden change from the M to a paramagnetic insu-

lator (PI) phase at $T = T_0$ in the range 190–385K; the transition temperature T_0 decreases with increasing x. Thus the stability range of the metallic phase diminishes with increasing Al or Cr content; simultaneously, the metallic resistivity increases with x by 2 orders of magnitude over the range $0.005 \leq x \leq 0.018$. Finally, there is an enormous hysteresis of approximately 50–70K which accompanies the M–PI transformation. As the temperature is raised further, the resistivity of the PI phase diminishes gradually until a lower plateau is reached which very nearly matches the resistivity of undoped V_2O_3 beyond 800K. In this region the PI gradually gives way to a second metallic phase, M′.

III. For more heavily doped alloys $(V_{1-x}M_x)_2O_3$, with M = Cr, Al and $0.018 \leq x \leq 0.10$, one encounters two transformations. At low temperature the material is an antiferromagnetic insulator; a small AFI–PI transition occurs between 160 and 180K depending on alloy composition. With further increases in temperature the M′ phase is ultimately reached beyond 800K. Thus the metallic phase of regimes I and II is missing.

IV. The $(V_{1-x}Ti_x)_2O_3$ system displays characteristics quite similar to those of I, except that the AFI–M phase transformation temperature is sharply reduced, and the size of the resistivity discontinuity is diminished, with increasing Ti content. For $x \gtrsim 0.055$ the M–AFI discontinuity disappears altogether.

V. This regime encompasses the nonstoichiometric oxide $V_{2(1-y)}O_3$ which is known to involve cation vacancies. Here again the AFI–M transition temperature diminishes rapidly with increasing y. The size of the resistivity discontinuity increases by approximately 4 orders of magnitude and for $y \gtrsim 0.009$ the transition disappears altogether.

VI. For the alloys $(V_{1-x}Ti_x)_2O_3$, with $0.055 < x < 0.1$, or $V_{2(1-y)}O_3$, $0.009 < y < 0.035$, all transitions have been eliminated; these materials are metallic, with resistivities roughly 4 orders of magnitude greater than those in conventional metals. However, it has recently been shown (*56*) that samples in this grouping undergo antiferromagnetic ordering at approximately 10K.

A review of Fig. 4 thus shows that in the alloy system $(V_{2-x}M_x)_2O_3$, with M = Cr, Al, T, or for $V_{2(1-y)}O_3$ and above 30K one encounters zero, one, two, or three distinct transitions depending on circumstances. All of the above transformations are also accompanied by anomalies or abrupt alterations of properties such as heat capacity, Seebeck coefficient, magnetic susceptibility, optical characteristics, and structural parameters. Lack of space precludes detailed consideration of these other effects. It is remarkable that small changes in composition can bring about such a wide variety of transitions and that the latter are triggered by as gentle a perturbation as a rise in temperature.

A very large number of mechanisms have been proposed to account for the above-mentioned transitions; for a somewhat dated review see Ref. (*1*) and other references therein. Many of the schemes were proposed before a complete set of investigations was available, and therefore are no longer viable. A recent proposal (*55*) which appears qualitatively consistent with the above facts is based on several band structure calculations (*57, 58*) which show that the density-of-states (DOS) curve for the d band in V_2O_3 exhibits a set of very high peaks and deep valleys in close alternation. The Fermi level is in close proximity to one of these very deep minima. It is postulated in Ref. (*55*) that this minimum may be replaced by a band gap which can be opened up by a variety of mechanisms: The first is the addition of diluents. Let the temperature be held fixed and allow the lattice to be diluted by an addition of Al or of Cr, so that one moves along the line aa' in Fig. 4. The

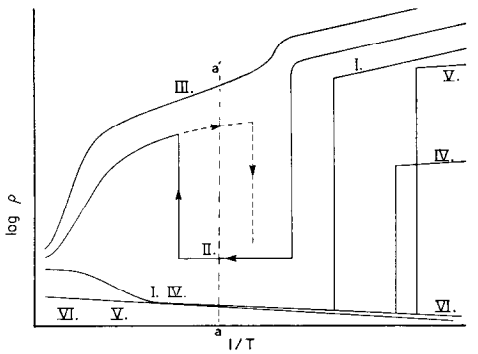

FIG. 4. Schematic diagram showing various types of electrical behavior in V_2O_3. For a discussion of regimes I–VI, see text.

Al *d* levels are thermally inaccessible; likewise, the Cr^{3+} state is characterized by extremely tightly bound electrons, rendering this state also inaccessible to fluctuations in electron density. The replacement of V and of its electron complement by Al or by the tightly bound Cr complex deprives the remaining electrons in the V_2O_3 host lattice of residence sites. This is equivalent to a dilution effect which narrows the *d* band, and which deepens the valley in the DOS curve. Since the electrical conductivity is proportional to the density-of-states at the Fermi level a deepening of the minimum lowers the conductivity. Ultimately, the minimum is superseded by a band gap and the material becomes an insulator. This accounts qualitatively for the rise in resistivity at fixed temperature with x in $(V_{2-x}M_x)_2O_3$ alloys, with M = Cr, Al and $0.005 < x < 0.018$. One finally reaches the regime $(V_{1-x}M_x)_2O_3$, with M = Cr, Al and $0.018 < x < 0.10$, for which the M phase is entirely absent.

Second, a band gap may open up for alloys of fixed composition $(V_{2-x}M_x)_2O_3$, with M = Cr, Al and $0.005 < x < 0.018$, when raising the temperature. The driving mechanism is the lowering of all occupied electron states near the Fermi level when the gap appears at the M–PI transition. This transformation is also accompanied by atomic rearrangements without change of symmetry (*59*), leading to a 1.5% increase in the unit volume. The gap has been estimated to be 0.3 eV (*55*). As the temperature is raised further, electrons are thermally promoted across this gap, which process leads to an energetic instability. To counteract the energy increase the gap closes gradually and ultimately is eliminated, so that one reverts to the M′ phase which is structurally and electrically very similar to the M phase. The gradual gap closure can be monitored by structural relaxation effects (*59*), as well as by a study of X-ray photoelectron spectroscopy (*60, 61*). The latter shows quite clearly the Fermi level intersecting the *d* band in the M phase, a free-standing Fermi level in the gap of the PI phase right after the transition, and a gradual reversion to the metallic phase beyond 800K. Thus the above scheme accounts for the high-temperature transitions for regimes II and III.

Third, a band gap may be opened up by magnetic order; for, the establishment of antiferromagnetism is accompanied by a symmetry change from rhombohedral to monoclinic. This again produces a rearrangement of energy states in the vicinity of the Fermi level, and results in opening up the same band gap as before, but this time due to a combination of symmetry reduction and unit cell doubling. One thereby accounts for the M–AFI transformation at low temperatures.

The transitions discussed so far have required that the Fermi level remain essentially at a constant position on the energy scale. This is the case so long as V and its electron complement are replaced by Al or Cr. However, when either excess oxygen or when titanium is incorporated the electron population is diminished, and the Fermi level moves away from its original position within the band gap or the minimum of the DOS curve. Ultimately, for $(V_{1-x}Ti_x)_2O_3$ alloys with sufficient Ti, or for

V_2O_3 sufficiently far removed from stoichiometry, the Fermi level will be out of reach of any band gap that might potentially develop. Such alloys do not exhibit any transitions and thus fall into category VI. In the intermediate range the magnetic ordering effects are expected to be increasingly perturbed by the addition of Ti or of excess O. Hence the M–AFI temperature should drop, which accords with the properties of alloys in regimes IV and V.

The above discussion is intended to show that a very simple model can cope with the experimental data summarized in Fig. 4. One should regard this model as a zero-order theory; for a more detailed understanding it is important to take account of electron correlation effects, electron phonon interactions, and of electron magnon interactions to achieve a more satisfactory description.

Acknowledgments

The author wishes to thank Professor J. Appel for many fruitful discussions. The reviews pertaining to Fe_3O_4, V_3O_5, and V_2O_3 were supported, respectively, by NSF Grants DMR81-03041, DMR79-08356, and NSF-MRL Grant DMR80-20249.

References

1. J. M. Honig and L. L. Van Zandt, *in* "Annual Review of Materials Sciences" (R. A. Huggins, R. H. Bube, and R. W. Roberts, Eds.), Vol. 5, pp. 225 ff, and references therein to earlier reviews. Annual Reviews, Palo Alto, CA (1975).
2. N. F. Mott, *Physics Today* **31,** 42 (1978).
3. *Phil. Mag. B* **42,** No. 10, October 1980.
4. E. J. Samuelsen, E. J. Bleeker, L. Dobrzynski, and T. Riste, *J. Appl. Phys.* **39,** 1114 (1968).
5. Y. Fujii, G. Shirane, and Y. Yamada, *Phys. Rev. B* **11,** 2036 (1975).
6. M. Iizumi and G. Shirane, *Solid State Commun.* **17,** 433 (1975).
7. S. M. Shapiro, M. Iizumi, and G. Shirane, *Phys. Rev. B* **14,** 200 (1976).
8. S. Iida, K. Mizuchima, M. Mizoguchi, S. Uemura, and J. Yoshida, *J. Appl. Phys.* **49,** 1456 (1978).
9. M. Mizoguchi, *J. Phys. Soc. Japan* **44,** 1512 (1978).
10. J. R. Cullen, *Phil. Mag. B* **42,** 387 (1980).
11. S. Iida, *Phil. Mag. B* **42,** 349 (1980).
12. Y. Yamada, *Ferroelectrics* **16,** 49 (1977).
13. N. W. Ashcroft and N. D. Mermin, "Solid State Physics," Chp. 33, Holt, Rinehart, and Winston, New York (1976).
14. N. F. Mott, *Festkörperprobleme* (J. Treusch, Ed.), Vol. 19, pp. 331 ff, Vieweg, Braunschweig (1979).
15. N. F. Mott, *Phil. Mag. B* **42,** 327 (1980).
16. J. R. Cullen and E. R. Callen, *Phys. Rev. B* **7,** 397 (1973).
17. W. J. Siemons, *IBM J. Res. Rev.* **14,** 245 (1970).
18. B. A. Calhoun, *Phys. Rev.* **94,** 1577 (1954).
19. C. Constantin and M. Rosenberg, *Solid State Commun.* **9,** 675 (1971); AIP **10,** 1389 (1972), AIP Conference Proceedings Magn. & Magn. Mat. (E. K. D. Graham Jr. and J. J. Rhyne, Eds.), Vol. 10, pp. 1389 ff, American Institute of Physics, New York (1973).
20. A. J. M. Kuipers and V. A. M. Brabers, *Phys. Rev. B* **14,** 1401 (1976); *Phys. Rev. B* **20,** 594 (1979).
21. H. Graener, M. Rosenberg, T. E. Whall, and M. R. B. Jones, *Phil. Mag. B* **40,** 389 (1979).
22. W. R. McKinnon, C. M. Hurd, and I. Shiozaki, *J. Phys. C: Solid State Phys.* **14,** L877 (1981).
23. I. Shiozaki, C. M. Hurd, S. P. McAlister, W. R. McKinnon and P. Strobel, *J. Phys. C: Solid State Phys.* **14,** 4641 (1981).
24. D. Ihle and B. Lorenz, *Phil. Mag. B* **42,** 337 (1980).
25. M. Pai, D. Buttrey, and J. M. Honig, unpublished data.
26. M. Pai and J. M. Honig, *Phys. Stat. Sol. B* **108,** K79 (1981).
27. L. A. Bursill and B. G. Hyde, *in* "Progress in Solid State Chemistry" (H. Reiss and J. O. McCaldin, Eds.), Vol. 7, pp. 202 ff, Pergamon, Oxford (1972).
28. A. C. Gossard, F. J. DiSalvo, L. C. Erich, J. P. Remeika, H. Yasuoka, K. Kosuge, and S. Kachi, *Phys. Rev. B* **10,** 4178 (1974).
29. H. V. Keer and J. M. Honig, *Mat. Res. Bull.* **12,** 277 (1977).
30. H. Okinaka, K. Kosuge, S. Kachi, M. Takano, and T. Takada, *J. Phys. Soc. Japan* **32,** 1148 (1972).
31. A. Heidemann, *Phys. Stat. Sol. A* **16,** K129 (1973).
32. A. Heidemann, K. Kosuge, and S. Kachi, *Phys. Stat. Sol. A* **35,** 481 (1976).

33. H. JHANS AND J. M. HONIG, *J. Solid State Chem.* **38,** 112 (1981).
34. E. I. TERUKOV, H. WAGNER, W. REICHELT, AND H. OPPERMANN, *Phys. Stat. Sol. A* **44,** K187 (1977).
35. F. A. CHUDNOVSKII, E. I. TERUKOV, AND D. I. KHOMSKII, *Solid State Commun.* **25,** 573 (1978).
36. J. ASHKENAZI AND M. WEGER, *J. Phys (Paris)* **37,** C4-189 (1976).
37. C. CASTELLANI, C. R. NATOLI, AND J. RANNINGER, *Phys. Rev. B* **18,** 4945, 4967, 5001 (1978).
38. M. GUPTA, A. J. FREEMAN, AND D. E. ELLIS, *Phys. Rev. B* **16,** 3338 (1977).
39. S. ÄSBRINK, *Mat. Res. Bull.* **10,** 861 (1975); *Acta Cryst. B* **36,** 1332 (1980).
40. H. HORIUCHI, N. MORIMOTO, AND M. TOKONAMI, *J. Solid State Chem.* **17,** 407 (1976).
41. W. BRÜCKNER, W. MOLDENHAUER, B. THUSS, AND G. FÖRSTERLING, *Phys. Stat. Sol. A* **35,** K49 (1976).
42. S. ÅSBRINK AND S.-H. HONG, *Nature* **279,** 624 (1979).
43. N. N. KHOI, T. R. SIMON, AND H. K. EASTWOOD, *Mat. Res. Bull.* **11,** 873 (1976).
44. N. F. KARTENKO, E. I. TERUKOV, AND F. A. CHUDNOVSKII, *Fiz. Tverd. Tela* **18,** 1874 (1975) [*Soviet Physics-Solid State* **18,** 1092 (1976)].
45. S. NAGATA, B. F. GRIFFING, G. D. KHATTAK, AND P. H. KEESOM, *J. Appl. Phys.* **50,** 7575 (1979).
46. B. F. GRIFFING, S. P. FAILE, AND J. M. HONIG, *Phys. Rev. B* **21,** 154 (1980).
47. M. FISHER, *Phil. Mag.* **7,** 1731 (1962).
48. J. C. BONNER AND M. E. FISHER, *Phys. Rev.* **135A,** 640 (1964).
49. L. DE JONGH AND A. MIEDEMA, *Adv. Phys.* **23,** 1 (1974).
50. J. E. KEEM AND J. M. HONIG, *Phys. Stat. Sol. B* **28,** 335 (1975).
51. D. B. MCWHAN, A. JAYARAMAN, J. P. REMEIKA, AND T. M. RICE, *Phys. Rev. Letters* **34,** 574 (1975).
52. J. DUMAS AND C. SCHLENKER, *J. Phys. (Paris)* **37,** C4-41 (1976).
53. H. KUWAMOTO, H. V. KEER, J. E. KEEM, S. A. SHIVASHANKAR, L. L. VAN ZANDT, AND J. M. HONIG, *J. Phys. (Paris)* **37,** C4-35 (1976).
54. H. KUWAMOTO AND J. M. HONIG, *J. Solid State Chem.* **23,** 335 (1980).
55. H. KUWAMOTO, J. M. HONIG, AND J. APPEL, *Phys. Rev. B* **22,** 2626 (1980).
56. Y. UEDA, K. KOSUGE, AND S. KACHI, *J. Solid State Chem.* **31,** 171 (1980).
57. J. ASHKENAZI AND M. WEGER, *J. Phys. (Paris)* **37,** C4-189 (1976).
58. C. CASTELLANI, C. R. NATOLI, AND J. RANNINGER, *J. Phys. (Paris)* **37,** C4-199 (1976); *Phys. Rev. B* **18,** 4945, 4967, 5001 (1978).
59. W. R. ROBINSON, *Acta Cryst. B* **31,** 1153 (1975).
60. S. VASUDEVAN, M. S. HEGDE, AND C. N. R. RAO, *Solid State Comm.* **27,** 131 (1978).
61. M. S. HEDGE AND S. VASUDEVAN, *Pramana* **12,** 151 (1979).